Seismic response of three-dimensional alluvial valleys

La réponse sismique des vallées alluvionnaires en trois dimensions

L.E.PÉREZ-ROCHA, Centro de Investigación Sísmica, A.C., México, D.F., Mexico
F.J.SÁNCHEZ-SESMA, Centro de Investigación Sísmica, A.C., México, D.F., Mexico, and Instituto de Ingeniería, UNAM, CU, México, D.F., Mexico
S.CHÁVEZ-PÉREZ, Centro de Investigación Sísmica, A.C., México, D.F., Mexico

SYNOPSIS: A boundary method is applied to study the seismic response of three-dimensional alluvial valleys on the surface of an elastic half-space. The excitation is given by incidence of plane waves. The method makes use of wave function families which are solutions of the Navier equation. The refracted and scattered displacement fields are constructed with wave function linear forms. Coefficients are obtained from a least-squares point matching of boundary conditions. Axial symmetry of the valleys allows the use of an azimuthal decomposition, and the solution of the problem is feasible through superposition of several two-dimensional solutions. Results are presented for incidence of SH and Rayleigh waves in time domain. Large amplifications and spatial variation of ground motion are found in both cases, clearly indicating the significance of the phenomenon in earthquake analyses.

1 INTRODUCTION

It is a widely known fact that local site conditions can generate large amplifications and relevant spatial variations of seismic ground motion. Lateral heterogeneities on the ground surface, as well as in stratified soils, have been related to damage distribution produced by several earthquakes (Sánchez-Sesma, 1987). For instance, the recent September 19, 1985, Michoacán, México earthquake has been the most damaging event to date in Mexico City (Beck and Hall, 1986). Source and path effects (Singh et al., 1988), and resonance in the uppermost sediments of the valley greatly amplified the motion. Most of these effects can be generally explained through one-dimensional models of the seismic response of surficial strata on soft soil. However, the influence of two- and three-dimensional local site effects is still not well known, but certainly important in the soil mechanics, and engineering seismology contexts.

The seismic response of two-dimensional alluvial valleys has been studied by several investigators (e.g., Bard and Bouchon, 1980a, b, 1985; Sánchez-Sesma et al., 1988; Bravo et al., 1988) considering several types of incident waves and valley configurations. This has allowed to understand essential aspects of the problem. However, papers describing three-dimensional models are very few in number, mainly because of the inherent difficulties found in their treatment. Lee (1984) used wave function expansions, and Lee and Langston (1983) utilized ray theory to study axisymmetric valleys. For the same geometry, a recently developed boundary method utilizes wave function expansions and an azimuthal decomposition to reduce by one the dimensionality of this problem (Sánchez-Sesma, 1983; Sánchez-Sesma et al., 1984; Chávez-Pérez and Sánchez-Sesma, 1984). The general formulation showing its numerical advantages has been presented by Sánchez-Sesma (1983), but numerical results have only been reported for normally incident P and SV waves in the frequency domain.

The aim of this paper is to consider non-normal incidence of SH waves, as well as Rayleigh surface waves, in the seismic response analysis of three-dimensional alluvial valleys. The formulation of the method is summarized and the numerical solution briefly described. Results are given in time domain for the sake of showing the importance of this phenomenon, and its value for seismic risk evaluation in strong earthquake ground motion.

2 FOUNDATIONS OF THE METHOD

Let us consider a three-dimensional alluvial valley on the surface of an elastic half-space as shown in Figure 1. The half-space and the valley are denoted by E and R, respectively. Let $\partial_1 E$ and $\partial_1 R$ be the free boundaries of the regions, and $\partial_2 E = \partial_2 R$ the common boundary between them. For harmonic time dependence, the displacement vector u must satisfy the reduced Navier equation

$$\mu\nabla^2 \mathbf{u} + (\lambda+\mu)\nabla\nabla\cdot\mathbf{u} + \rho\omega^2\mathbf{u} = 0, \qquad (1)$$

where λ and μ = Lamé constants, ρ = mass density, ω = circular frequency, and ∇ = gradient operator.

Under incidence of elastic waves, the total displacement field in the exterior region E is obtained by superposition of scattered waves on the free-field solution (i.e., the solution in absence of surficial imperfections). In region R, the solution is given by refracted waves. Boundary conditions are those of zero tractions

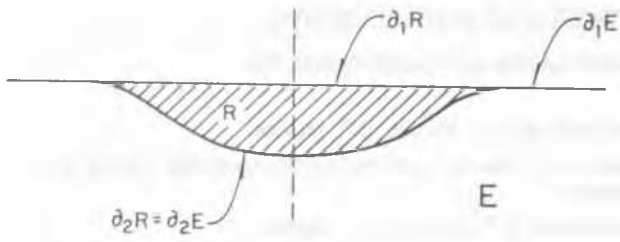

Figure 1. Definition of regions E and R, and their boundaries.

at $\partial_1 E$ and $\partial_1 R$, and continuity of displacements and tractions across $\partial_2 E = \partial_2 R$. In addition, the scattered fields must satisfy the elastic radiation condition at infinity, which means that no energy may be radiated from infinity into the prescribed singularities of the field. Then, let us write the total field in region E by means of

$$u^E = u^{(0)} + u^{(s)}, \quad (2)$$

where $u^{(0)}$= free-field solution displacement vector, and $u^{(s)}$= scattered field displacement vector given by

$$u^{(s)} = \sum_{j=0}^{2} \sum_{n=0}^{N} \sum_{m=0}^{n} A_{jnm} W^E_{jnm}. \quad (3)$$

For region R, we have

$$u^R = \sum_{j=0}^{2} \sum_{n=0}^{M} \sum_{m=0}^{n} B_{jnm} W^R_{jnm}. \quad (4)$$

For the latter two equations, W^E_{jnm} are displacement vectors of the scattered fields, and W^R_{jnm} are displacement vectors of the refracted fields, respectively. A_{jnm} and B_{jnm} are unknown coefficients, and N and M are the orders of the expansions. The range of values for j (= 0, 1, 2) stands for the types of waves involved; namely, toroidal SH waves, and spheroidal P and SV waves, respectively. The solutions depend on two other indexes; n and m, the radial and azimuthal numbers, respectively. The diffracted and refracted solutions can, in general, be written in the form

$$f_n(r)\ F^m_n(\theta, \phi), \quad (5)$$

where $f_n(r)$, the radial function, is given in terms of spherical Hankel or Bessel functions for the regions E or R, respectively (Sánchez-Sesma, 1983). $F^m_n(\theta, \phi)$ is a vector function given in its different forms in terms of the surface spherical function (e.g., Takeuchi and Saito, 1972)

$$Y^m_n(\theta, \phi) = P^m_n(\cos\theta)\ e^{im\phi} \quad (6)$$

and its derivatives. Here, $P^m_n(\cdot)$ = associated Legendre function, and m = 0, ±1, ±2,..., ±n.

It should be pointed out that each one of the displacements vectors W^E_{jnm}, does not satisfy in itself the free-boundary conditions on the half-space surface. Because of this, the numerical treatment is extended to part of the free-surface, but this is not a serious restriction. For the range of frequencies covered in this work, it suffices to take twice or three times the half-width of the valley to obtain good results.

The numerical solution is carried out by imposing boundary conditions at a finite number of points on the boundaries. This yields to a system of linear equations for the unknown coefficients (the independent part is given in terms of the free-field solution), which is solved in the least-squares sense. Once the coefficients are known, equations 2, 3, and 4 allow us to calculate the displacement fields at any point of the regions E and R, and their boundaries. This collocation method or point matching approach has been useful to perform two-dimensional computations (Sánchez-Sesma et al.,1982, 1985).

3 THE AZIMUTHAL DECOMPOSITION

If the shape of the irregularity is independent of the spherical coordinate ϕ, its axisymmetry with respect to the z-axis, and the orthogonality of all the azimuthal functions, grant a complete decomposition of the problem in terms of the azimuthal number. It can be shown that any component of the free-field can be expanded in a Fourier series of azimuthal functions (Sánchez-Sesma, 1983). In spherical coordinates (Figure 2), these components acquire oddness and eveness properties with respect to the azimuthal angle which are also applicable to the scattered and refracted fields. For instance, it can be seen, from equations 3 to 6, that the scattered and refracted fields contain sinus and cosinus of $m\phi$, where ϕ = azimuthal angle. Therefore, if the scatterer is axiymmetric, boundary conditions also have these properties, and it suffices to solve a "two-dimensional" problem for each azimuthal number in the r, θ spherical coordinates. The final solution is attained by superposing each partial result.

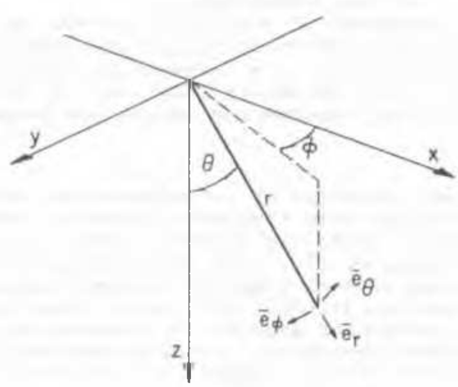

Figure 2. Cartesian and spherical coordinate systems. Unit vectors in the spherical system.

For normally incident plane waves, only one azimuthal number is needed. In this case, for P waves, only m = 0 is required; for SV and SH waves, it suffices to take m = 1. For almost grazing incidences, or Rayleigh waves with large horizontal wavenumbers, this approach requires many azimuthal numbers. However, even in this critical case, four or five azimuthal terms give a good approximation if the horizontal wavelengths of the incident field are of the order of the maximum horizontal dimension of the irregularity.

4 NUMERICAL EXAMPLES

Results in frequency domain are given in terms of the normalized frequency

$$\eta = \frac{\omega a}{\pi \beta_E}, \qquad (7)$$

where $\beta_E = \sqrt{\mu/\rho}$ = shear wave velocity of the half-space, and a = radius of the valley. For time domain results, the Fast Fourier Transform algorithm is used to compute the convolution of the transfer function, given by the total solution for several normalized frequencies, and the frequency spectrum of the assumed source wavelet. We utilize a Ricker wavelet defined by

$$f(t) = (A-B)\exp(-A), \qquad (8)$$

where $A = \pi^2(t-t_s)^2/t_p^2$, $B = \pi^2 t_s^2/t_p^2$, t_s/t_p = 0.1983, and t_p = "characteristic period".

The order of the expansions, and the number and location of collocation points are obtained using a "trial and error" procedure based upon the error analysis of boundary conditions and the stability of the calculated surface displacement fields. The order of the expansions we utilized for the scattered fields is roughly given by $N \approx 4(1+\eta^2)^{-1}+13\eta$, whereas for the refracted fields is given by $M \approx 4(1+\eta^2)^{-1}+15\eta$.

The maximum azimuthal number used is of about $(2+7\eta)/2$, but never less than 2. The number of collocation points is of about 30η, but never less than 8. They were placed uniformly at $\partial_1 R$, $\partial_2 R$, and at $\partial_1 E$ in a length of 2a. In all the computations, the residual tractions and displacements did not exceed the six per cent of maximum free-field stresses and displacements, respectively. Typically, when these residual errors are lower than this value, the calculations for several analyses do not show significant changes.

Figure 3 displays results of the three-dimensional response of a semispherical alluvial valley under oblique incidence of SH waves of unit amplitude. The geometry of the valley is the simplest one we can investigate with our method. This selection has been made to support the fact that shear wave responses are valuable for seismic risk evaluation and show the feasibility of their three-dimensional computations. Synthetic seismograms, given by the total solution up to a value η = 2, are shown at nine surface receivers for the horizontal displacement component u_y. Important spatial variations in ground motion are observed, and large amplications are found, mainly in the central region of the valley, of up to 500 per cent.

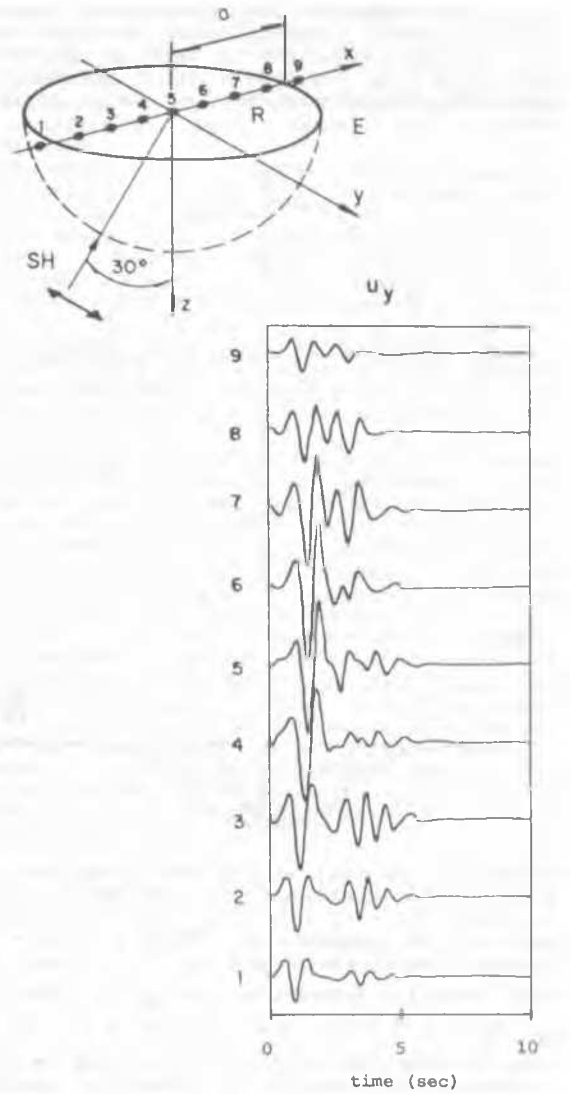

Figure. 3. Response of a semispherical alluvial valley with radius a = 700 m to an obliquely incident SH Ricker wavelet of "characteristic" period t_p = 1.0 sec. Poisson coefficients are ν_R = 0.3 and ν_E = 0.25. Material properties are μ_R/μ_E = 0.2, $\rho_R = \rho_E$, β_E = 2.1 km/s, and β_R/β_E = 0.45. Traces represent displacements (u_y component) at nine surface receivers marked with dots in the upper part.

On the other hand, it is also a well known fact that strong ground motion contains significant contributions from surface waves. Then, let us consider impinging Rayleigh waves of unit amplitude upon another kind of alluvial valley (Figure 4). Synthetic seismograms, given by the total solution up to a value η = 3, are shown in Figures 5 and 6 for two different sections. In Figure 5, u_y = 0 because of the symmetry of the problem. Large amplifications are observed, mainly in the vertical displacement component u_z, and surface waves seem to be present. By studying the particle motion, we find that it is retrograde at the beginning of the synthetics. This suggests the presence of emergent Rayleigh waves. Figure 6 also displays important spatial variations in vertical ground motion. Also note the emergence of the non-incident displacement component u_y due to converted waves.

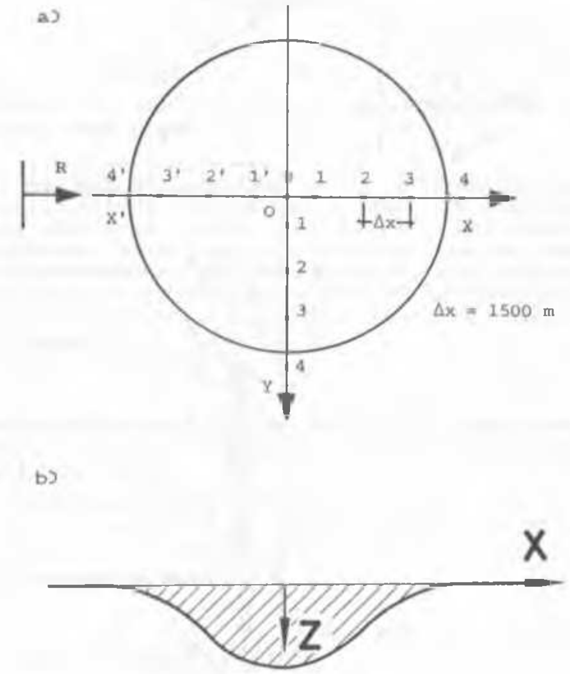

Figure 4. Alluvial valley with interface shape given by the equation $z = h(1-3\xi^2+2\xi^3)$, $0 \le \xi \le 1$, where $\xi = (x^2+y^2)^{1/2}/a$, and h = maximum depth of the deposit. a = 5000 m. h/a = 0.5. Poisson coefficients are ν_R = 0.3 and ν_E = 0.25. Material properties are μ_R/μ_E = 0.3, $\rho_R = \rho_E$, β_E = 1.5 km/s, and β_R/β_E = 0.71. a) Plan view showing the location of surface receivers in sections X'X and OY. R stands for incidence of Rayleigh waves. b) Cross section.

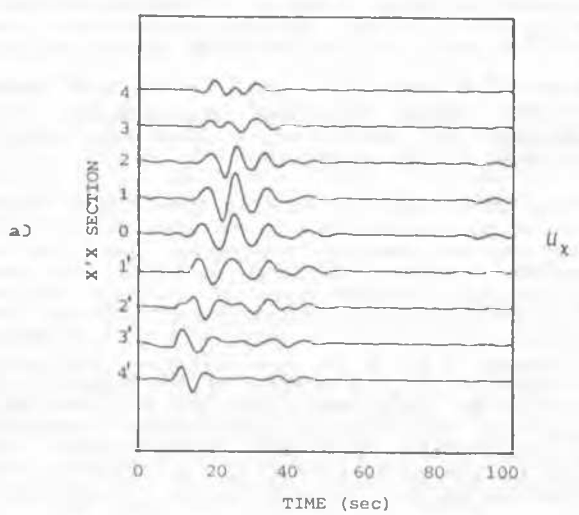

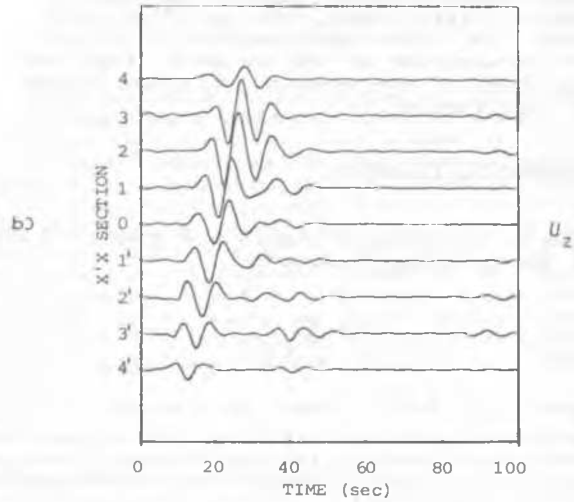

Figure 5. Synthetic seismograms for the displacement components (a) u_x and (b) u_z in section X'X under incident Rayleigh waves upon the alluvial valley of Figure 4. Ricker wavelet of "characteristic" period t_p = 12 sec.

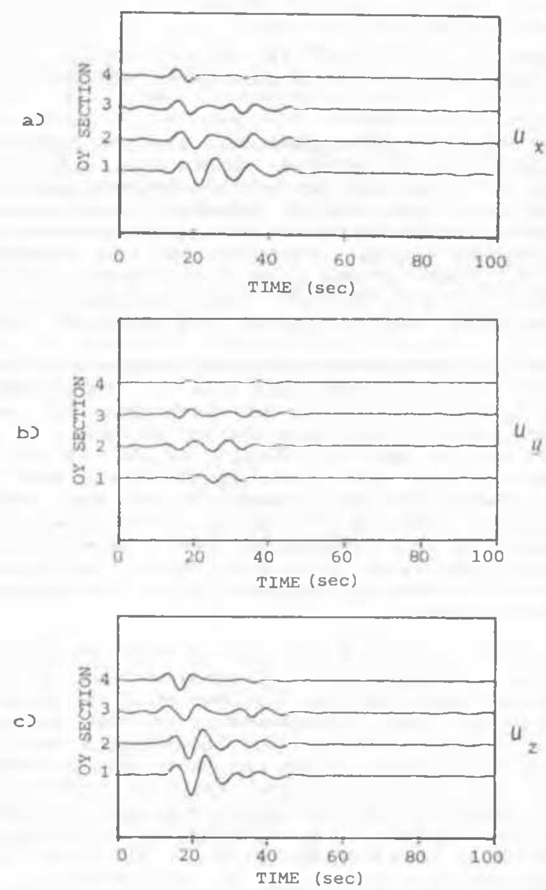

Figure 6. Synthetic seismograms for the displacement components (a) u_x, (b) u_y, and (c) u_z in section OY under incident Rayleigh waves upon the alluvial valley of Figure 4. Ricker wavelet of "characteristic" period t_p = 12 sec.

5 CONCLUSIONS

(1) A boundary method has been applied to study the seismic response of three-dimensional alluvial valleys in time domain. Axisymmetric scatterers are assumed to allow an azimuthal decomposition of the problem, and reduce by one its dimensionality. The solution is obtained by superposing a sequence of "two-dimensional" problems.

(2) Results for the oblique incidence of *SH* body waves and Rayleigh surface waves upon two kinds of alluvial valleys show large amplifications associated with three-dimensional effects which increase the complexity and spatial variation of ground motion.

(3) This work demonstrates the feasibility of quantitative three-dimensional studies of local site response. The method furnishes an alternative way to calibrate other procedures and can also be extended to study the dynamic response of foundations.

ACKNOWLEDGMENTS

Parts of this work were performed at the Institut de Recherches Interdisciplinaires en Géologie et Mécanique de l'Université Joseph Fourier de Grenoble, France, and at the Department of Geological Sciences, Univ. of Southern California, USA. We wish to thank K. Aki, P.-Y. Bard, M.A. Bravo, M. Campillo, and J.-C. Gariel for helpful discussions. Financial support has been provided by National Science Foundation (USA) under grant EAR-8610905, and Consejo Nacional de Ciencia y Tecnología (México).

REFERENCES

Bard, P.-Y. and M. Bouchon (1980a). The seismic response of sediment-filled valleys. Part 1. The case of incident SH waves, Bull. Seism. Soc. Am. 70. 1263-1286.
Bard, P.-Y. and M. Bouchon (1980b). The seismic response of sediment-filled valleys. Part 2. The case of incident P and SV waves, Bull. Seism. Soc. Am. 70, 1921-1941.
Bard, P.-Y. and M. Bouchon (1985). The two-dimensional resonance of sediment-filled valleys, Bull. Seism. Soc. Am. 75, 519-542.
Beck, J.L. and J.F. Hall (1986). Factors contributing to the catastrophe in Mexico City during the earthquake of September 19, 1985, Geophys. Res. Lett. 13, 593-596.
Bravo, M.A., F.J. Sánchez-Sesma, and F.J. Chávez-García (1988). Ground motion on stratified alluvial deposits for incident SH waves, Bull. Seism. Soc. Am. 78, 436-450.
Chávez-Pérez, S. and F.J. Sánchez-Sesma (1984). Ground motion on three-dimensional topographies under incident P, SV and Rayleigh waves (abstract), Earthquake Notes 55, 13.
Lee, V.W. (1984). Three-dimensional diffraction of plane P, SV & SH waves by a hemispherical alluvial valley, Soil Dyn. Earthquake Eng. 3, 133-144.
Lee, J.J. and C.A. Langston (1983). Wave propagation in a three-dimensional circular basin, Bull. Seism. Soc. Am. 73, 1637-1655.
Sánchez-Sesma, F.J. (1983). Diffraction of elastic waves by three-dimensional surface irregularities, Bull. Seism. Soc. Am. 73, 1621-1636.
Sánchez-Sesma, F.J. (1987). Site effects on strong ground motion, Int. J. Earthquake Eng. Struct. Dyn. 6, 124-132.
Sánchez-Sesma, F.J., I. Herrera, and J. Avilés (1982). A boundary method for elastic wave diffraction. Application to scattering of SH waves by surface irregularities, Bull. Seism. Soc. Am. 72, 473-490.
Sánchez-Sesma, F.J., S. Chávez-Pérez, and J. Avilés (1984). Scattering of elastic waves by three-dimensional topographies, Proc. 8th World Conf. Earthquake Eng. 2, 639-646, San Francisco.
Sánchez-Sesma, F.J., M.A. Bravo, and I. Herrera (1985). Surface motion of topographical irregularities for incident P, SV, and Rayleigh waves, Bull. Seism. Soc. Am. 75, 263-269.
Sánchez-Sesma, F.J., F.J. Chávez-García, and M. A. Bravo (1988). Seismic response of a class of alluvial valleys for incident SH waves, Bull. Seism. Soc. Am. 78, 83-95.
Singh, S.K., E. Mena, and R. Castro (1988). Some aspects of source characteristics of the 19 September 1985 Michoacán earthquake and ground motion amplification in and near Mexico City from strong motion data, Bull. Seism. Soc. Am. 78, 451-477.
Takeuchi, H. and M. Saito (1972). Seismic surface waves, in Methods in computational physics 11, B. A. Bolt, editor, Academic Press, Inc., New York.